

Department of Applied Geology

**Quantification of an Archaean to Recent
Earth Expansion Process Using Global
Geological and Geophysical Data Sets**

James Maxlow

This thesis is presented as part of the
requirement for the award of the
Doctor of Philosophy
of
Curtin University of Technology

June 2001

CONTENTS Volume 2 of 2

	Page
APPENDICES	
A1. KINEMATICS OF EARTH EXPANSION	1
A1.1 Radius, Circumference, Surface Area, Volume	2
A1.2 Mass Density and Surface Gravity	3
A1.3 Secular Rate of Earth expansion	4
A2. SPACE GEODETIC CHARTS	6
A2.1 VLBI Space Geodetic Charts	8
A2.2 SLR Space Geodetic Charts	42
A2.3 GPS Space Geodetic Charts	83
A2.4 LLR Space Geodetic Chart	98
A3. PALAEOMAGNETIC FORMULAE	100
A3.1 Magnetic Dipole Equations	100
A3.2 Modified Dipole Formulae	104
A4. PALAEOMAGNETIC DATA	109
A5. PUBLICATIONS	195
A6. CD-ROM DISC Opening Instructions	222
(CD-ROM disc is stored in a sleeve located within the back cover of this volume)	

LIST OF FIGURES

Figure A3.1 Geocentric axial dipole model.	100
Figure A3.2 Palaeopoles determined using the conventional dipole equation.	102
Figure A3.3 Determining the actual palaeopole position on the present Earth.	103
Figure A3.4 Determination of a magnetic pole from a magnetic field direction.	105
Figure A3.5 Ellipse of confidence about a magnetic pole position.	107

LIST OF TABLES

Table A1.1 Empirical surface area data derived from Larson <i>et al.</i> (1985).	1
Table A1.2 Derived quantities for the variables radius, circumference, surface area and volume	2

A1. KINEMATICS OF EARTH EXPANSION

An investigation into the kinematics of an Earth expansion with time uses the equation for palaeoradius:

$$R_a = (R_0 - R_p)e^{kt} + R_p \quad (\text{Equation 2.6})$$

which was derived in Section 2.2 from empirical oceanic surface area data (Table A1.1) and continental surface area based on a primordial Earth of radius 1700 kilometres. Equation 2.6 is a mathematical expression for exponential change in the palaeoradius of the Earth from the Archaean to the Recent, and assumes that oceanic and continental lithosphere is fully fixed in the rock record with little or no requirement for removal of lithosphere by subduction.

Table A1.1 Empirical surface area data derived from Larson *et al.* (1985). Areas digitized and calculated using a CAD based Graphical Design System software package. Arbitrarily assigned errors are $\pm 5\%$ (from Maxlow, 1995).

Age		Surface Area			Palaeoradius
Chron	Years ($\times 10^6$)	dS ($\times 10^7$ km ²)	Σ dS ($\times 10^7$ km ²)	$S_a = S_0 - \Sigma$ dS ($\times 10^7$ km ²)	R_a (km)
0	0	0	0	51.0000	6370.80
C2	0-1.9	0.5342	0.5342	50.4658	6337.15
C3a	1.9-5.9	1.3328	1.8670	49.3300	6265.43
C6b	5.9-23.0	4.9213	6.7883	44.2117	5931.49
C15	23.0-37.7	4.1624	10.9507	40.0493	5645.37
C25	37.7-59.2	4.1649	15.1156	35.8844	5343.77
C29	59.2-66.2	1.0462	16.1618	34.8382	5265.30
C34	66.2-84.0	4.7956	20.9574	30.0426	4889.49
M0	84.0-118.7	5.6758	26.6332	24.3668	4403.46
M17	118.7-143.8	1.9348	28.5680	22.4320	4225.02
M38	143.8-205	1.9386	30.5066	20.4934	4038.31

S_0 = present surface area = 5.1×10^8 km² (Stacey, 1977), S_a = ancient surface area, dS = surface area of chron interval, Σ dS = cumulative chron interval surface areas, R_a = ancient palaeoradius.

Known parameters of the present Earth at time t_0 are (Stacey, 1977):

$$R_0 = 6.3708 \times 10^6 \text{ m}$$

$$S_0 = 5.1000 \times 10^{14} \text{ m}^2$$

$$V_0 = 1.0830 \times 10^{21} \text{ m}^3$$

$$M_0 = 5.9730 \times 10^{24} \text{ kg}$$

$$D_0 = 5.5150 \times 10^3 \text{ kg/m}^3$$

$$G_0 = 6.6732 \times 10^{-11} \text{ m}^3 \text{ kg}^{-1} \text{ sec}^{-2}$$

$$g_0 = 9.780317 \text{ m sec}^{-2}$$

Where: R = palaeoradius, S = surface area, V = volume, M = mass, D = mean density, G = universal gravitation, g = surface gravity of the Earth

A1.1 Radius, Circumference, Surface Area, Volume

Derived quantities for the variables radius, circumference, surface area and volume are calculated for the time interval t_0 (present) to t_{3800} (Archaean) using the following equations:

$$\text{Ancient Radius} \quad R_a = (R_0 - R_p)e^{kt} + R_p$$

$$\text{Ancient Circumference} \quad C_a = 2\pi R_a = 2\pi((R_0 - R_p)e^{kt} + R_p)$$

$$\text{Ancient Surface Area} \quad S_a = 4\pi R_a^2 = 4\pi((R_0 - R_p)e^{kt} + R_p)^2$$

$$\text{Ancient Volume} \quad V_a = (4/3)\pi(R_a)^3 = (4/3)\pi((R_0 - R_p)e^{kt} + R_p)^3$$

Where: R_a = past Earth palaeoradius, R_0 = present mean Earth radius = 6370.8 km (Stacey 1977), R_p = primordial Earth radius = 1700 km, e = an exponent, $k = 4.5366 \times 10^{-9}$ /year (Section 2.2), t = time before present (negative)

Derived quantities for radius, circumference, surface area and volume are listed in Table A1.2 and shown in Figure 2.7 (Section 2.3).

Table A1.2 Derived quantities for the variables radius, circumference, surface area and volume. Calculated from palaeoradius Equation 2.6.

Geologic Time Scale		Kinematics			
Chron	Age	Radius	Circumference	Area	Volume
	(m.y.)	(km)	(kmx10 ⁴)	(km ² x10 ⁵)	(km ³ x10 ⁸)
Future	300	19916.4	12513.81	49845.91	330916.26
Future	200	13272.8	8339.54	22137.79	97943.42
Future	100	9052.2	5687.64	10297.07	31070.24
Future	5	6478.0	4070.22	5273.35	11386.84
C0 Present	0.0	6370.8	4002.89	5100.32	10831.05
C2 Quaternary	-1.9	6330.7	3977.70	5036.34	10627.87
C3A Pliocene	-5.9	6247.4	3925.38	4904.72	10213.97
C6B Miocene	-23.0	5908.0	3712.11	4386.23	8637.94
C15 Oligocene	-37.7	5636.5	3541.54	3992.39	7501.08
C25 Eocene	-59.2	5270.7	3311.68	3490.97	6133.29
C29 Paleocene	-66.2	5159.1	3241.55	3344.69	5751.85
C34 Late Cretaceous	-84.0	4890.7	3072.94	3005.79	4900.19
M0 Mid Cretaceous	-118.7	4426.0	2780.93	2461.68	3631.79
M17 Early Cretaceous	-143.8	4132.6	2596.59	2146.14	2956.38
M29 Late Jurassic	-160.0	3960.2	2488.29	1970.84	2601.67
M38 Early Jurassic	-205.0	3542.9	2226.05	1577.32	1862.74
Triassic	-245.0	3237.0	2033.89	1316.75	1420.79
Permian	-286.0	2976.2	1869.98	1113.07	1104.22
Carboniferous	-360.0	2612.2	1641.32	857.50	746.66
Devonian	-408.0	2433.7	1529.16	744.31	603.82
Silurian	-438.0	2340.4	1470.50	688.30	536.96
Ordovician	-505.0	2172.5	1365.04	593.11	429.52
Cambrian	-570.0	2051.9	1289.22	529.06	361.85
Neoproterozoic	-900.0	1778.7	1117.61	397.59	235.74
Mesoproterozoic	-1,600.0	1703.3	1070.21	364.57	206.99
Palaeoproterozoic	-2,500.0	1700.1	1068.18	363.19	205.82
Archaean	-3,800.0	1700.0	1068.14	363.17	205.8

A1.2 Mass Density and Surface Gravity

The kinematics of mass, density and surface gravity, assuming a simplistic spherical Earth model with a homogeneous mass and density distribution is governed by the standard equations:

$$\text{Density} \quad D = \text{Mass} / \text{Volume}$$

and:

$$\text{Surface gravity} \quad g = GM/R^2$$

In the density equation, volume is calculated from Equation 2.6 and the variables mass M and density D are unknown. In the surface gravity equation, universal gravitation G is assumed to be constant. Three possible scenarios exist for an expression representing the kinematics of mass, density and surface gravity with time:

1. Mass remains constant requiring density to decrease exponentially as volume increases throughout geological time.
2. Density remains constant requiring mass to increase exponentially as volume increases throughout geological time.
3. Both mass and density are variable as volume increases throughout geological time.

Derived quantities for the variables mass, density and surface gravity for conditions of a) constant mass and b) constant density are calculated by incorporating Equation 2.6 for the time interval t_0 to t_{3800} using the following equations:

a) Constant Mass: $M = M_0$
 $D = M/V = M_0 / (4/3)\pi((R_0 - R_p)e^{kt} + R_p)^3$
 $g = GM/R^2 = GM_0 / ((R_0 - R_p)e^{kt} + R_p)^2$

b) Constant Density: $D = D_0$
 $M = DV = D_0(4/3)\pi((R_0 - R_p)e^{kt} + R_p)^3$
 $g = GM/R^2 = GD_0(4/3)\pi((R_0 - R_p)e^{kt} + R_p)^3 / ((R_0 - R_p)e^{kt} + R_p)^2$
 $= GD_0(4/3)\pi((R_0 - R_p)e^{kt} + R_p)$

Each of these variables is shown graphically in Figure 2.8 (Section 2.3).

A1.3 Secular Rate of Earth expansion

The secular rate of Earth expansion is defined as an incremental increase in the physical dimensions of the Earth throughout geological time and may be quantified by considering the variables radius, circumference, surface area and volume. Mass, density and surface gravity are considered speculative and mass is assumed to

increase with time (Section 2.3). The application of Equation 2.6 enables the secular rate of Earth expansion to be determined for the following variables between times t_1 and t_2 :

$$dR/dt = (R_1 - R_2)/(t_1 - t_2) = (((R_0 - R_p)e^{kt_1} + R_p) - ((R_0 - R_p)e^{kt_2} + R_p))/(t_1 - t_2)$$

$$dC/dt = (C_1 - C_2)/(t_1 - t_2) = ((2\pi((R_0 - R_p)e^{kt_1} + R_p)) - (2\pi((R_0 - R_p)e^{kt_2} + R_p)))/(t_1 - t_2)$$

$$dS/dt = (S_1 - S_2)/(t_1 - t_2) = ((4\pi((R_0 - R_p)e^{kt_1} + R_p)^2) - (4\pi((R_0 - R_p)e^{kt_2} + R_p)^2))/(t_1 - t_2)$$

$$dV/dt = (V_1 - V_2)/(t_1 - t_2) = ((4\pi/3)((R_0 - R_p)e^{kt_1} + R_p)^3 - (4\pi/3)((R_0 - R_p)e^{kt_2} + R_p)^3)/(t_1 - t_2)$$

Assuming a constant Earth density and variable mass and surface gravity:

$$dD/dt = 0$$

$$dM/dt = (M_1 - M_2)/(t_1 - t_2)$$

$$= (D_0(4/3)\pi((R_0 - R_p)e^{kt_1} + R_p)^3 - D_0(4/3)\pi((R_0 - R_p)e^{kt_2} + R_p)^3)/(t_1 - t_2)$$

$$dg/dt = (g_1 - g_2)/(t_1 - t_2)$$

$$= (GD_0(4/3)\pi((R_0 - R_p)e^{kt_1} + R_p)^3 - GD_0(4/3)\pi((R_0 - R_p)e^{kt_2} + R_p)^3)/(t_1 - t_2)$$

The present secular rates of Earth expansion derived from the above formulae at time t_0 are:

Radius	$dR/dt_0 = 22 \text{ mm/year}$
Circumference	$dC/dt_0 = 140 \text{ mm/year}$
Surface Area	$dS/dt_0 = 3.50 \text{ km}^2/\text{year}$
Volume	$dV/dt_0 = 11,000 \text{ km}^3/\text{year}$
Mass	$dM/dt_0 = 60 \times 10^{12} \text{ tonnes/year}$
Density	$dD/dt_0 = 0$
Surface Gravity	$dg/dt_0 = 3.4 \times 10^{-8} \text{ msec}^{-2}/\text{year}$

A2. SPACE GEODETIC CHARTS

The following contains charted and tabulated information on 88 VLBI, SLR, GPS and LLR observation sites used by the International Earth Rotation Service (ITRF) during the period 1992 to 1997 inclusive. Charts are organised into Appendix A2.1: VLBI; Appendix A2.2: SLR; Appendix A2.3: GPS and; Appendix A2.4: LLR. Within each appendix, charts are arranged in numerical order according to the observation site location number. Charts represent plots of the variation of actual Earth radius of a particular observing site, derived from published International Earth Rotation Service geodetic solutions for 1992, 1993, 1994, 1996 and 1997 (<http://lareg.ensg.ign.fr/ITRF/>). Site position geocentric co-ordinates and velocity vectors for VLBI, SLR, GPS and LLR (one observation only) solutions are tabulated with each chart. Graphs shown on all charts represent plots of Earth radii relative to the geocentric centre of the Earth for each year of publication, followed by radii derived from published velocity vectors projected in yearly increments to 1999.

Earth radii are derived using the following equation:

$$\text{Earth radius} = \sqrt{X^2 + Y^2 + Z^2} \quad (\text{Equation A2.1})$$

Where: X, Y, and Z represent the published site co-ordinates in ITRF cartesian co-ordinates relative to the centre of the Earth's mass.

Projected time variant Earth radii are derived using:

$$\text{Projected Earth radius} = \sqrt{(X+V_x)^2 + (Y+V_y)^2 + (Z+V_z)^2} \quad (\text{Equation A2.2})$$

Where: V_x , V_y , and V_z represent the published site velocities in ITRF cartesian co-ordinates relative to the centre of the Earth's mass.

Predicted Earth expansion is derived using:

$$\text{Earth radius} = \sqrt{X^2 + Y^2 + Z^2} + 0.022 \quad (\text{Equation A2.3})$$

Where: 0.022 represents the radial increase in Earth expansion in millimetres per year determined from Equation 2.6 (Section 2.2, and Appendix A1).

For each chart the 1992 solution is adopted as a starting point for plotting predicted Earth expansion. Actual radius variation is shown as a thick line by joining the published solutions for each year shown. For each of the VLBI sites in Appendix 2.1, GSFC solution 1102g 1998 is also included for reference only. Part of this VLBI solution is constrained within the ITRF97 global solution.

A2.1 VLBI Space Geodetic Charts

A2.2 SLR Space Geodetic Charts

A2.3 GPS Space Geodetic Charts

A2.4 LLR Space Geodetic Chart

A3. PALAEO-MAGNETIC FORMULAE

A3.1 Magnetic Dipole Equations

The geocentric axial dipole model is central to the principles of palaeomagnetism (Figure A3.1). In this conventional Earth model a magnetic field produced by a single magnetic dipole \mathbf{M} , located at the centre of the Earth and aligned with the rotation axis, is considered.

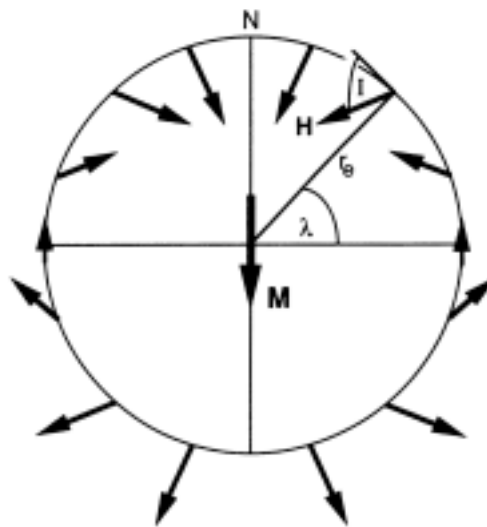


Figure A3.1. Geocentric axial dipole model. A magnetic dipole \mathbf{M} is located at the centre of the Earth and aligned with the rotation axis. The geographic latitude is λ , the mean Earth radius is r_e , the magnetic field directions at the Earth's surface, produced by the geocentric axial dipole are schematically shown, inclination \mathbf{I} is shown for one location and \mathbf{N} is the North geographic pole. (from Butler, 1992)

The derivation of the conventional dipole equation is given in Butler (1992) and defined as:

$$\tan \mathbf{I} = 2 \tan \lambda = 2 \cot p \quad (\text{Equation A3.1})$$

Where:

\mathbf{I} is the mean inclination of the magnetic field, increasing from -90° at the geographic south pole to $+90^\circ$ at the geographic north pole

λ is the geographic latitude determined from \mathbf{I}

p is the geographic colatitude determined from \mathbf{I}

Rearranging the dipole equation gives colatitude p as:

$$p = \cot^{-1} (\tan I/2) = \tan^{-1} (2/\tan I) \quad (\text{Equation A3.2})$$

Equation A3.2 represents a measure of the great-circle angular distance from the mean sample site to the magnetic pole and, like latitude is independent of any radial or time constraints imposed by the sample. The dipole equation is a general equation applicable to any sized magnetic sphere that obeys the geocentric axial dipole model (Figure A3.1). On this sphere the magnetic lines of force behave in exactly the same manner, irrespective of scale and, for a given site inclination, the colatitude (or latitude) calculated using the dipole equation will always remain the same.

Figure A3.2 demonstrates this very important characteristic of the dipole equation where, for a given site value I , the dipole equation remains true for an infinite number of sites along a radius vector R , passing through the centre of the Earth to the site location and beyond. Colatitude (Equation A3.2) calculated from an inclination I at sites S_1, \dots, S_n , located along the radius vector R , is equal to a constant angular measurement p . At site S_1 this colatitude p represents an arcuate distance D_1 which is not equal to distances D_2, \dots, D_n for sites S_2, \dots, S_n using the identical values of inclination I and colatitude p .

For a simplistic radial expansion of the Earth from R_1 to R_2, \dots, R_n the palaeopole positions P_1, P_2, \dots, P_n calculated from the conventional dipole equation (Equation A3.2) are shown (Figure A3.2). Because the conventional dipole equation uses angular measurements and has no provision for either a radial or time component to compensate for the shift in actual palaeopole position with expansion, the calculated pole positions will always coincide with the geomagnetic pole N .

To determine the ancient palaeopole position P_a on the present day Earth with palaeoradius varying exponentially with time, consider Figure A3.3. At site S_0 located at the present radius R_0 , using the conventional palaeocolatitude equation (Equation A3.2) an inclination I gives a colatitude p_0 which equates with the palaeocolatitude p_a locked into the rock record from site S_a at palaeoradius R_a .

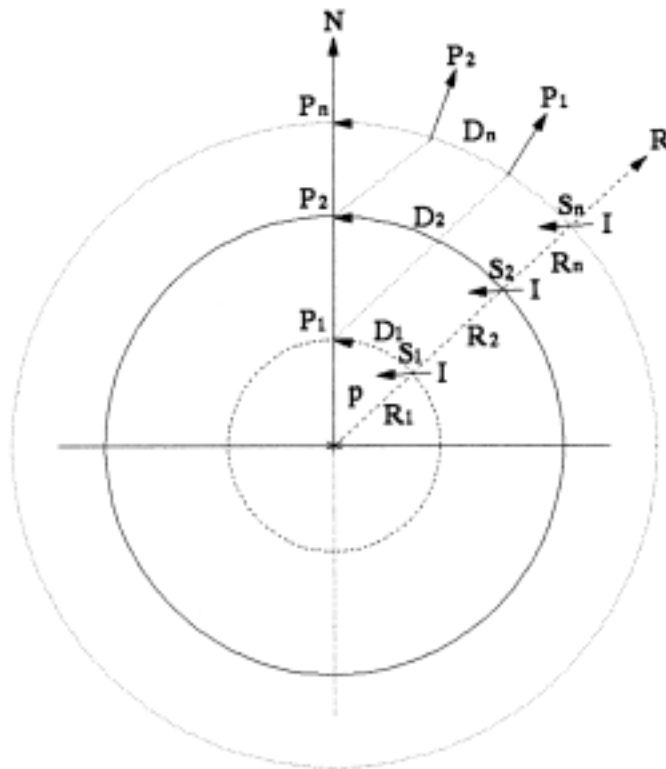


Figure A3.2. Palaeopoles determined using the conventional dipole equation. Cross section showing a number geocentric axial dipolar spheres. For a given site value I the dipole equation remains true for an infinite number of sample sites S_1 to S_n along a radius vector R . The colatitude calculated from inclination I at sites S_1 to S_n is equal to a constant angular measurement p . At sites S_1 this colatitude p represents an arcuate distance D_1 which is not equal to distances D_2 to D_n for sites S_2 to S_n . No provision is made in the dipole equation for a variation in palaeoradius with time in determining the actual palaeopole positions P_1 to P_n .

At site S_a the arc distance D_a is equal to:

$$D_a = R_a p_a$$

Where p_a is in radians. Rearranging:

$$p_a = (D_a/R_a)$$

To determine the palaeopole position P_a located on the present radius Earth, which equates to the ancient palaeopole position P_a determined from site S_a , palaeocolatitude:

$$p = (D_a/R_0) \times 180/\pi = (R_a p_a \times (\pi/180)/R_0) \times 180/\pi = R_a p_a / R_0$$

Where p is in degrees.

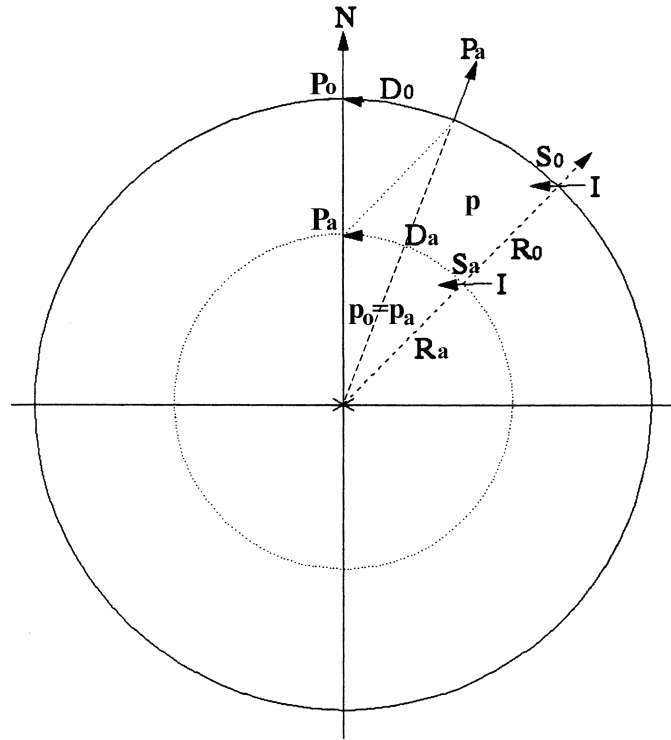


Figure A3.3. Determining the actual palaeopole position on the present Earth. Cross section shows an ancient Earth at palaeoradius R_a and a present Earth at present radius R_0 . For an inclination I , site S_0 , and present radius R_0 , the arcuate distance to palaeopole P is D_0 , and colatitude p_0 . For site S_a , palaeoradius R_a and arcuate distance D_a , the colatitude p_a is the same for site S_0 , but the actual palaeopole position on the present Earth is located at position P_a determined from D_a .

The mathematical relationship for an exponential increase in the Earth's palaeoradius, derived from empirical measurements of oceanic and continental surface area data was previously found to be (Equation 2.6) (Section 2.3):

$$R_a = (R_0 - R_p)e^{kt} + R_p \quad (\text{Equation 2.6})$$

Incorporating Equation 2.6 for R_a gives:

$$p = ((R_0 - R_p)e^{kt} + R_p)p_a/R_0$$

and incorporating Equation A4.2 for p_a gives:

$$p = ((R_0 - R_p)e^{kt} + R_p) (\tan^{-1} (2/\tan I))/R_0$$

For any site sample, constrained by the age of the rock sequence containing the site data, the palaeocolatitude from site to the ancient palaeopole position on an Earth of present radius is equal to:

$$p = ((R_0 - R_p)e^{kt} + R_p) (\tan^{-1} (2/\tan I))/R_0 \quad (\text{Equation A3.3})$$

The application of this modified dipole equation to palaeomagnetic site data (Section 3.2.2) enables palaeocolatitude to be converted to the present geographical grid system. This correctly locates the ancient palaeopole position on the present Earth. To determine palaeolatitude and establish latitudinal zonation, the conventional dipole equation (Equation A3.2) is used.

The modified dipole Equation A3.3 can now be used to develop formulae to convert ancient palaeopole geographical coordinates to present geographical coordinates from ancient site mean data located on the present Earth. This enables palaeopoles to be correctly located on the present Earth, constrained by both time and palaeoradius.

A3.2 Modified Dipole Formulae

Site mean data determined from a set of site samples are assumed by palaeomagneticians to represent a time-averaged field which compensates for any secular variation caused by non-dipole components (Tarling, 1983). For a geocentric axial dipole field (Figure A3.1) the time-averaged and structurally corrected inclination I , determined from site data establishes the palaeocolatitude existing at the site when the site data were locked into the rock-record and a time-average declination D determines the direction along a palaeomeridian to the palaeopole.

Calculation of the palaeomagnetic pole position on the present Earth surface uses spherical trigonometry, based on the dipole Equation 3.1, to determine the distance traveled from the observing locality to the pole position (Figure A3.4).

Details and derivation of the following conventional palaeomagnetic equations, sign conventions and symbols for geographic locations, are adopted from Butler (1992):

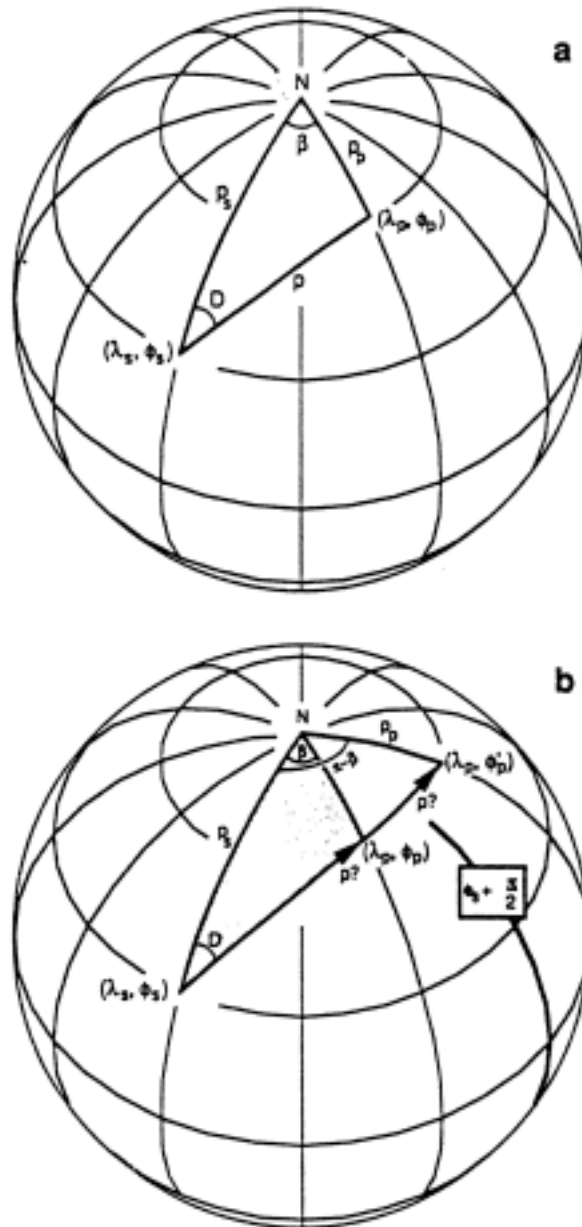


Figure A3.4. Determination of a magnetic pole from a magnetic field direction, using the palaeomagnetic dipole equation. Orthorhombic projection with latitude and longitude grid in 30° increments. Figure A3.4a: the site latitude and longitude is (λ_s, ϕ_s) ; the palaeomagnetic pole is located at (λ_p, ϕ_p) ; site colatitude is p_s ; colatitude of the magnetic pole is p_p ; and the longitudinal difference between the magnetic pole and site is β . Figure A3.4b: illustrates the ambiguity in magnetic pole longitude. The pole may be at either (λ_p, ϕ_p) or (λ_p, ϕ'_p) ; the longitude at $\phi_s + \pi/2$ is shown by the heavy meridian line. (From Butler, 1992).

- latitudes increase from -90° at the south geographic pole to 0° at the equator and $+90^\circ$ at the north geographic pole;
- longitudes east of the Greenwich meridian are positive, while westerly longitudes are negative and;
- (λ_p, ϕ_p) is the pole position calculated from a site-mean direction (I_m, D_m) measured at site location (λ_s, ϕ_s) .

The pole latitude derived from spherical trigonometry (Figure A3.4) is:

$$\lambda_p = \sin^{-1} (\sin\lambda_s \cos p + \cos\lambda_s \sin p \cos D_m) \quad (\text{Equation A3.4})$$

The longitudinal difference between pole and site, denoted by β , is positive towards the east, negative towards the west and is:

$$\beta = \sin^{-1} (\sin p \sin D_m / \cos\lambda_p) \quad (\text{Equation A3.5})$$

where if:

$$\cos p \geq \sin\lambda_s \sin\lambda_p \quad (\text{Equation A3.6})$$

then the pole longitude:

$$\phi_p = \phi_s + \beta \quad (\text{Equation A3.7})$$

but if:

$$\cos p \leq \sin\lambda_s \sin\lambda_p \quad (\text{Equation A3.8})$$

then the pole longitude:

$$\phi_p = \phi_s + 180^\circ - \beta \quad (\text{Equation A3.9})$$

For any site-mean direction (I_m, D_m) the associated circular confidence limit (α_{95}) is transformed into an ellipse of confidence about the calculated pole position with semi-axes of angular length given by (Figure A3.5):

$$d_p = \alpha_{95} ((1 + 3\cos^2 p)/2) = 2 \alpha_{95} (1 / (1 + 3\cos^2 I_m)) \quad (\text{Equation A3.10})$$

and:

$$d_m = \alpha_{95} (\sin p / \cos I_m) \quad (\text{Equation A3.11})$$

While Equations A3.4 to A3.11 represent the basis for conventional plate tectonic determination of pole positions and derived apparent polar wander paths, they do not and cannot acknowledge any variation in angular dimension of palaeogeographical grids as a result of a variable palaeoradius or time constraint. What is assumed by these equations is that the angular dimension of the palaeogeographical co-ordinate system, indicated by the site-data, equals the angular dimension of the geographical co-ordinate system represented by the present site location. By using these conventional palaeomagnetic equations to determine the palaeopole position the two systems are then simply added, using spherical trigonometry to give a palaeopole latitude and longitude.

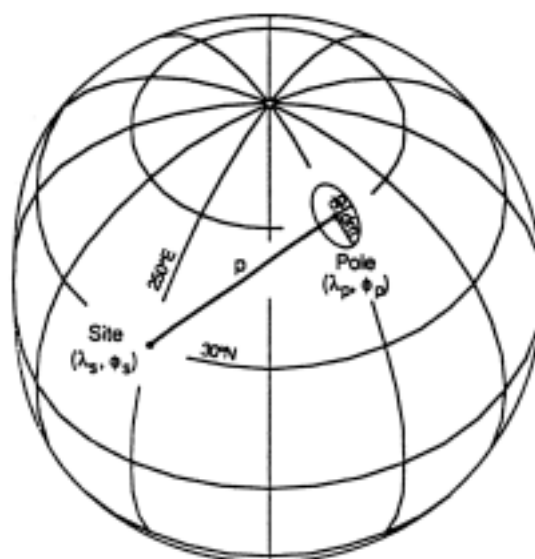


Figure A3.5. Ellipse of confidence about a magnetic pole position, determined using the palaeomagnetic dipole equation. For a magnetic colatitude p , d_p is the semi-axis of a confidence ellipse along the great-circle path from site to pole; d_m is the semi-axis perpendicular to that great-circle path. Orthorhombic projection, with latitude and longitude grid in 30° increments. (From Butler, 1992)

To determine actual palaeopole locations on the present Earth each site sample must be qualified by a time constraint to convert the palaeogeographical co-ordinate system to the present system. For an Earth undergoing an exponential increase in palaeoradius from the Archaean to the Recent, derivation of palaeocolatitude from site data is (Equation A3.3):

$$\mathbf{p} = ((\mathbf{R}_0 - \mathbf{R}_p)e^{kt} + \mathbf{R}_p) (\tan^{-1} (2/\tan I))/\mathbf{R}_0 \quad (\text{Equation A3.3})$$

By incorporating palaeocolatitude Equation A3.3 into the pole coordinate Equations A3.4 to A3.11 of Butler (1992), equations that constrain the palaeocolatitude arcuate distances to the present geographical co-ordinates are established. These are then used to determine the actual palaeopole location on the present Earth surface.

Palaeopole latitude becomes:

$$\lambda_p = \sin^{-1} (\sin\lambda_s \cos[(\mathbf{R}_0 - \mathbf{R}_p)e^{kt} + \mathbf{R}_p] (\tan^{-1} (2/\tan I))/\mathbf{R}_0] + \cos\lambda_s \sin[(\mathbf{R}_0 - \mathbf{R}_p)e^{kt} + \mathbf{R}_p] (\tan^{-1} (2/\tan I))/\mathbf{R}_0] \cos D_m) \quad (\text{Equation A3.12})$$

longitudinal difference becomes:

$$\beta = \sin^{-1} (\sin[(\mathbf{R}_0 - \mathbf{R}_p)e^{kt} + \mathbf{R}_p] (\tan^{-1} (2/\tan I))/\mathbf{R}_0] \sin D_m / \cos\lambda_p) \quad (\text{Equation A3.13})$$

where if:

$$\cos[(\mathbf{R}_0 - \mathbf{R}_p)e^{kt} + \mathbf{R}_p] (\tan^{-1} (2/\tan I))/\mathbf{R}_0] \geq \sin\lambda_s \sin\lambda_p \quad (\text{Equation A3.14})$$

then the palaeopole longitude:

$$\phi_p = \phi_s + \beta \quad (\text{Equation A3.15})$$

but if:

$$\cos[(\mathbf{R}_0 - \mathbf{R}_p)e^{kt} + \mathbf{R}_p] (\tan^{-1} (2/\tan I))/\mathbf{R}_0] \leq \sin\lambda_s \sin\lambda_p \quad (\text{Equation A3.16})$$

then the palaeopole longitude:

$$\phi_p = \phi_s + 180^\circ - \beta \quad (\text{Equation A3.17})$$

and ellipse of confidence:

$$\begin{aligned}
 \mathbf{d}_p &= \alpha_{95} ((1 + 3\cos^2[(\mathbf{R}_0 - \mathbf{R}_p)e^{kt} + \mathbf{R}_p]) (\tan^{-1} (2/\tan \mathbf{I}))/\mathbf{R}_0)/2 \\
 &= 2 \alpha_{95} (1/ (1 + 3\cos^2 \mathbf{I}_m))
 \end{aligned}
 \tag{Equation A3.18}$$

and:

$$\mathbf{d}_m = \alpha_{95} (\sin[(\mathbf{R}_0 - \mathbf{R}_p)e^{kt} + \mathbf{R}_p]) (\tan^{-1} (2/\tan \mathbf{I}))/\mathbf{R}_0/\cos\mathbf{I}_m \tag{Equation A3.19}$$

A4. PALAEOMAGNETIC DATA

Actual palaeopole locations derived from the structurally corrected palaeomagnetic data of McElhinny & Lock (1996) using modified palaeomagnetic Equations A3.12 to A3.19.

	Page
Table A4.1 Recent Palaeomagnetic Data	110
Table A4.2 Pliocene Palaeomagnetic Data	123
Table A4.3 Miocene Palaeomagnetic Data	125
Table A4.4 Oligocene Palaeomagnetic Data	129
Table A4.5 Eocene Palaeomagnetic Data	132
Table A4.6 Paleocene Palaeomagnetic Data	136
Table A4.7 Late Cretaceous Palaeomagnetic Data	137
Table A4.8 Mid Cretaceous Palaeomagnetic Data	141
Table A4.9 Early Cretaceous Palaeomagnetic Data	146
Table A4.10 Late Jurassic Palaeomagnetic Data	149
Table A4.11 Early Jurassic Palaeomagnetic Data	151
Table A4.12 Triassic Palaeomagnetic Data	155
Table A4.13 Permian Palaeomagnetic Data	159
Table A4.14 Carboniferous Palaeomagnetic Data	166
Table A4.15 Devonian Palaeomagnetic Data	172
Table A4.16 Silurian Palaeomagnetic Data	176
Table A4.17 Ordovician Palaeomagnetic Data	178
Table A4.18 Cambrian Palaeomagnetic Data	183
Table A4.19 Neoproterozoic Palaeomagnetic Data	185
Table A4.20 Mesoproterozoic Palaeomagnetic Data	188
Table A4.21 Palaeoproterozoic Palaeomagnetic Data	191
Table A4.22 Archaean Palaeomagnetic Data	194

A5. PUBLICATIONS

- MAXLOW J. 1998. Global expansion tectonics: Empirical small Earth modelling of an exponentially expanding Earth. *Proceedings of International Symposium on New Concepts in Global Tectonics, 1998, Tsukuba, Japan*, 159-164.
- MAXLOW J. 2000a. Earth expansion: Quantification using Oceanic magnetic isochron mapping. *Himalayan Geology* **23**, 1-14.
- MAXLOW J. 2000b. Global Expansion Tectonics. *Nexus New Times Magazine* **7/6**, 41-46.

A6. CD-ROM DISC Opening Instructions

The attached CD-ROM disc contains video animations of selected figures from Volume 1 of 2. These animations were created from a series of GIF images and assembled as video clips in Adobe Premier version 5.0 at 640 x 480 pixel frame size, 24 fps frame rate and saved as MPG files. The Video animations use the same numbering system as the figures shown in the text volume, except the word Figure is replaced by Video and the number is prefaced by the letter A, eg. Figure 3.15 becomes Video A3.15. To run these video animations a computer with a Pentium II, 330 Mhz processor or better, 32 Mb of RAM and 16 Mb graphics card is required. At less than these specifications the animations will show erratic motion

To access the CD-ROM open in Microsoft Word (Word 97 or better) and open the file: **VideoClips.doc**. The animations will open within this document as embedded video clips and are activated by double clicking on the animation. The animation is controlled by a standard media player slide controller. Use the controller to stop the motion at any time and restart again as required.

LIST OF VIDEOS

- Video A1.1a** Recent to Permian spherical models of an expanding Earth.
- Video A1.1b** Permian to Archaean spherical models of an expanding Earth.
- Video A2.10** Archaean to Future spherical models of an expanding Earth.
- Video A2.13** Archaean-Mesoproterozoic expanding Earth model.
- Video A2.14** Four phases of expanding Earth developmental history.
- Video A2.31** The expanding Earth projected to 5 million years into the future.
- Video A3.5** Recent VLBI, SLR, GPS and DORIS horizontal plate motion.
- Video A3.13** Expanding Earth Archaean to Future palaeomagnetic north poles.
- Video A3.14** Expanding Earth Archaean to Future palaeomagnetic south poles.
- Video A3.15** Palaeogeography on an Archaean to Future expanding Earth.
- Video A3.15a** Palaeozoic palaeogeography.
- Video A3.15b** Mesozoic palaeogeography.
- Video A3.15c** Cenozoic palaeogeography.
- Video A3.18** Rodinia on a Late Neoproterozoic expanding Earth.
- Video A3.20** Gondwana on an Ordovician expanding Earth.

- Video A3.22** Pangaea on an Early Permian expanding Earth.
- Video A3.23** Triassic to Eocene Alpine-Himalayan orogenesis.
- Video A3.26** Mid- to Late-Cambrian agnostid trilobite and Early Ordovician platform trilobite faunas on an Ordovician expanding Earth.
- Video A3.27** Permian reptile and Mesozoic Dinosaurian locations on a Triassic expanding Earth.
- Video A3.28** New Zealand Middle and Late Jurassic marine taxa on a Late Jurassic expanding Earth.
- Video A3.29** *Glossopteris* flora on an Early Carboniferous expanding Earth.
- Video A3.30** Precambrian glacial deposits on a Neoproterozoic expanding Earth.
- Video A3.32** Early Palaeozoic glacial deposits on an Ordovician expanding Earth.
- Video A3.34** Late Palaeozoic glacial, carbonate and coal deposits on a Permian expanding Earth.
- Video A3.35** Late Palaeozoic to Triassic coal and Permo-Carboniferous carbonate reefs on a Permian expanding Earth.
- Video A3.36** Permo-Carboniferous to Triassic carbonate reefs plotted on an Early Jurassic expanding Earth.
- Video A3.37** Palaeozoic, Mesozoic, and Cenozoic oil and gas on a Mid Cretaceous expanding Earth.
- Video A3.38** Early to Late Cretaceous coal on a Late Cretaceous expanding Earth.
- Video A3.40** Precambrian metals on a Neoproterozoic expanding Earth.
- Video A3.41** Mid- to Late-Phanerozoic metals on an Early Jurassic expanding Earth.